Handbook on
ATMOSPHERIC DIFFUSION

Steven R. Hanna
Gary A. Briggs
Rayford P. Hosker, Jr.

Atmospheric Turbulence and Diffusion Laboratory
National Oceanic and Atmospheric Administration

This document is
PUBLICLY RELEASABLE

~~Barry Steele~~
Authorizing Official
Date: 5/18/04

Air-Pollution Meteorology in Complex Terrain

12-1 INTRODUCTION

In the past decade air-pollution meteorology in complex terrain has emerged as a top issue. Part of the reason for this is that many new power plants and other industries are being built in the mountainous western part of the United States. Furthermore, many eastern industries are located near hills and ridges, and recent regulations require that pollutant concentrations be calculated at the surface of these terrain obstacles. Interest is also inspired by the requirement to calculate the impact of sources on distant national parks and forest preserves.

Complex terrain influences the trajectory and the diffusion of a plume. Does the plume strike a ridge, or is it deflected above the ridge? What methods should be used to estimate diffusion? Field data necessary to answer these questions are seriously lacking. A few good field programs are now under way by the Environmental Protection Agency, the U. S. Department of Energy, and the Electric Power Research Institute. The techniques described in this chapter provide guidance for estimating diffusion in complex terrain.

12-2 METEOROLOGY

Even though it is possible that high-pollutant concentrations may occur in complex terrain (e.g., where plumes intercept hillsides), several physical processes are acting that tend to lower concentrations. The first of these is the tendency of wind to favor the "grain" of the terrain; it rarely goes across it. Many field studies show the validity of this statement. Figure 12.1 is a topographic map of the Widows Creek Steam Plant area in northeastern Alabama, where the major terrain obstacle is a linear 250-m terrain step. Figure 12.2 is a wind-rose diagram for meteorological stations in the valley and on the mountain (Hanna, 1980b). The wind on the mountain blows with nearly the same frequency from all directions, but the wind in the valley is strongly channeled up or down the valley, which reduces the probability of plume impingement on the mountain-side.

Another favorable meteorological effect in complex terrain is the enhancement of turbulence due to eddies that are set up by air passing over and around terrain obstacles. Panofsky, Egolf, and Lipschutz (1978) found that, for a meteorological tower 500 m downwind of a ridge, the standard deviation of wind-direction fluctuations (σ_θ) was increased by a factor of 2.5. Hanna (1980b) found that σ_θ was increased by a factor of 1.6 during neutral conditions when the wind direction was perpendicular to the valley (Fig. 12.1). The tower was located 2 to 10 km from the ridges to the northwest and southwest in Fig. 12.1. More detailed observations of σ_θ were made at a network of eleven towers in the Geysers, Calif., geothermal area. The terrain consists of randomly oriented 1000-m mountains and ridges. For the eleven stations, Hanna (1980c) calculated the median hourly σ_θ values from 5 days of observations at a height of 10 m. These σ_θ values are plotted against the hour of the day in Fig. 12.3, which shows that nighttime σ_θ values are about 20° to 26° and daytime values are about 30° to 35°. Over flat terrain nighttime σ_θ values are predicted to be only 5° or less (see Tables 4.2 and 4.3). With extreme stabilities, meandering may cause occasional high values of σ_θ. However, in the Geysers, σ_θ is consistently high for all stable conditions, which leads us to the conclusion that terrain obstacles cause an enhancement of σ_θ. This conclusion is further confirmed by the data in Fig. 12.4, in which σ_θ is plotted against wind speed for nighttime runs at a given station. At low wind speeds, corresponding to the largest static stability $[(g/T) \, \partial\theta/\partial z]$ at night, σ_θ is a maximum as a result of these terrain effects.

Of course, complex terrain also causes changes in surface-layer wind speed and direction which adversely affect pollutant concentrations. Pollutants emitted near the ground into the nighttime drainage
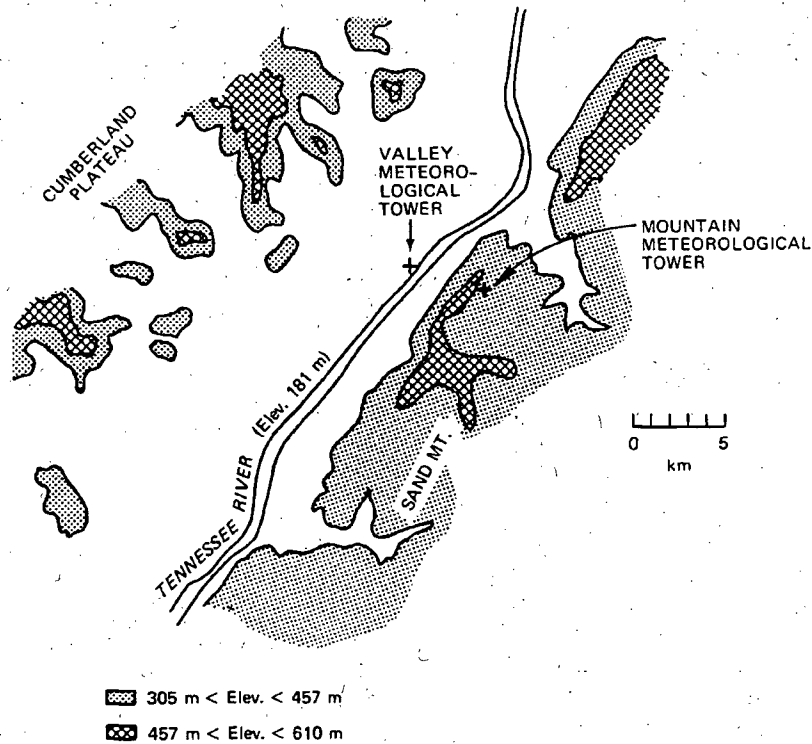
Fig. 12.1 Topographic map of area within 10 km of Widows Creek Steam Plant. Meteorological station locations are given.
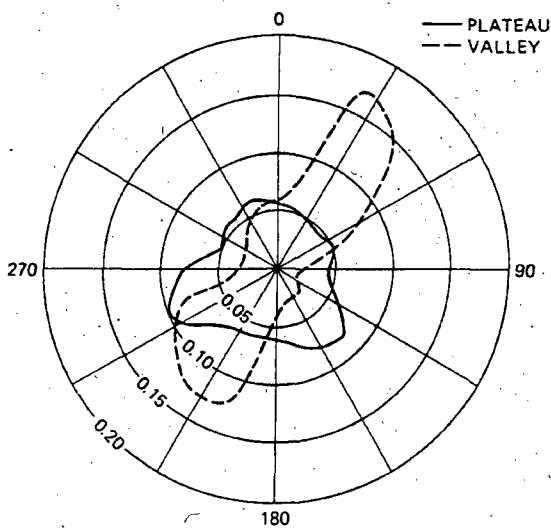

Fig. 12.2 Annual (1977) wind rose for valley and plateau meteorological stations (61-m level) at Widows Creek. Numbers are frequency per $22\frac{1}{2}°$ sector.

layer over sloping terrain may follow the drainage flow downhill toward population centers. The thickness (h) of the drainage layer on a simple slope is suggested by Briggs (1979) to be given by the formulas:

$$h = 0.05 \text{ x sin } \beta \qquad (\beta > 20°) \qquad (12.1)$$

$$h = 0.037 \text{ x } \beta^{\frac{2}{3}} \qquad (\beta < 20°) \qquad (12.2)$$

where x is the distance along the slope from the top of the slope and β is the slope angle in radians. For an angle of 20° and a distance of 500 m, the thickness (h) is about 9 m. Briggs (1979) used energy conservation principles to arrive at the following formula for the characteristic wind speed in the drainage layer:

$$u = 2.15(\sin \beta)^{\frac{2}{3}}(Hx)^{\frac{1}{3}} \qquad (12.3)$$

where H is the downward sensible heat flux (in units of m^2/sec^3), which is given by

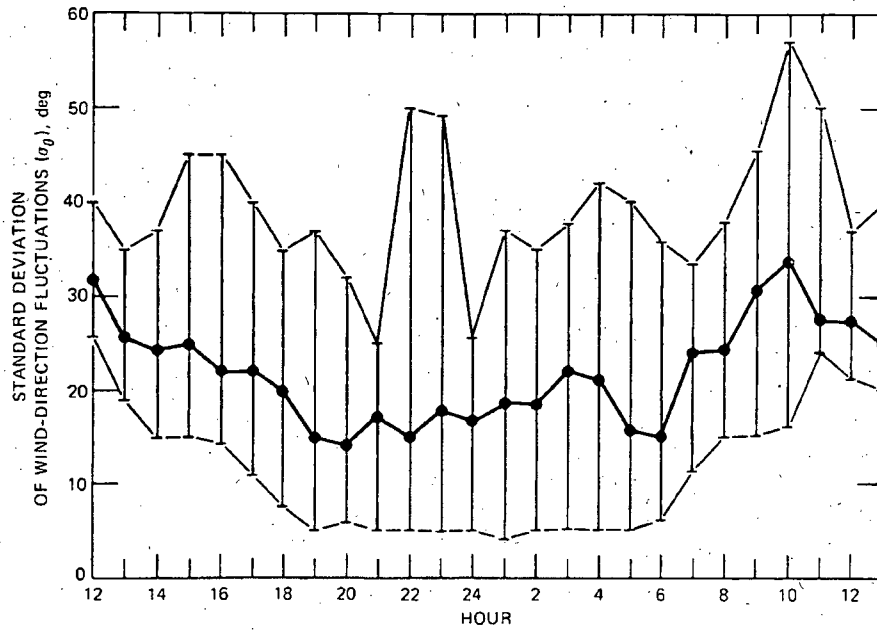$$H = -g \frac{\overline{w'T'}}{T} \qquad (12.4)$$

Fig. 12.3 Diurnal variation of σ_θ at a height of 10 m for 11 meteorological towers in complex terrain at the Geysers geothermal area. Hourly σ_θ values for 5 days were averaged together for each of 11 stations. The highest, median, and lowest of the 11 σ_θ values at each hour are plotted.
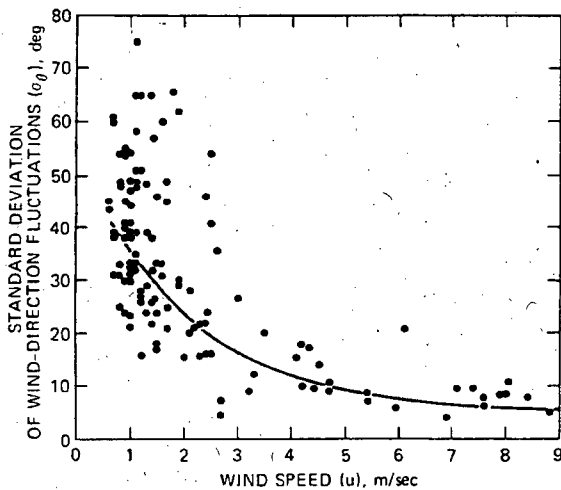

Fig. 12.4 Hourly average σ_θ vs. wind speed for nighttime (2100 to 0600) data from five observation nights at the Geysers geothermal area. This station is located about halfway down a 1000-m-elevation ridge.

For typical values, H can be of the order of 0.001 m^2/sec^3 on a clear night. If $\beta = 27°$ and x = 1 km, then u = 1.8 m/sec, which is a value of wind speed often observed in drainage layers. Drainage from the ideal slopes considered in the above derivation usually rises to converge into a narrower valley, which gives

a deeper drainage "river." An example of typical air trajectories in a valley is shown in Fig. 12.5, which is also taken from the results of the Geysers experiment (Nappo et al., 1980). This drainage flow has a depth of 50 to 100 m and a speed of 2 to 3 m/sec and is about 2 to 3 km downhill from the ridgetops. A few kilometers farther down the valley, where it broadens out and the slope decreases, the drainage pool is observed to be about 200 m deep with a speed of about 1 m/sec.

Numerical or physical models can be used to estimate wind flow over complex terrain. Most of the work before 1975 has been reported by Egan (1975). Numerical models in use are all "research-grade," and much developmental work needs to be done. The biggest need is for field data, which would aid in the development and testing of such models. In numerical models, it is difficult to obtain the necessary detail (small grid size) while still retaining a large enough domain size to cover the area of interest. For simple two-dimensional hills, the potential flow theory appears to give good results.

Physical models of flow over complex terrain have been reviewed by Hosker (1980), who points out that the most obvious effects occur when the flow is stratified. Blocking, lee waves, rotors, and wake formation are some of the more interesting

phenomena that have been observed. The stability parameter most often used to classify this work is the internal Froude number:

$$F_H \equiv \frac{U}{NH} \qquad (12.5)$$

where U is the free-stream wind speed, H is the hill height, and N is the Brunt–Väisälä frequency (in rads/sec):

$$N \equiv \left(\frac{g}{T}\frac{\partial \theta}{\partial z}\right)^{\frac{1}{2}} \qquad (12.6)$$

where θ is the potential temperature and N is the natural frequency of oscillation of an air parcel

displaced slightly in a stable atmosphere. For $F_H \leqslant 1$, motions tend to be limited to horizontal planes; i.e., plumes will impact the surface and try to go around hills rather than over them (Hunt, Snyder, and Lawson, 1978). For $F_H > 1$, the airflow is likely to be over the top of the hill.

12-3 · DIFFUSION CALCULATIONS

As Pasquill (1974) suggests, observations of wind flow and turbulence parameters, if available, should be used to calculate diffusion. However, in most real
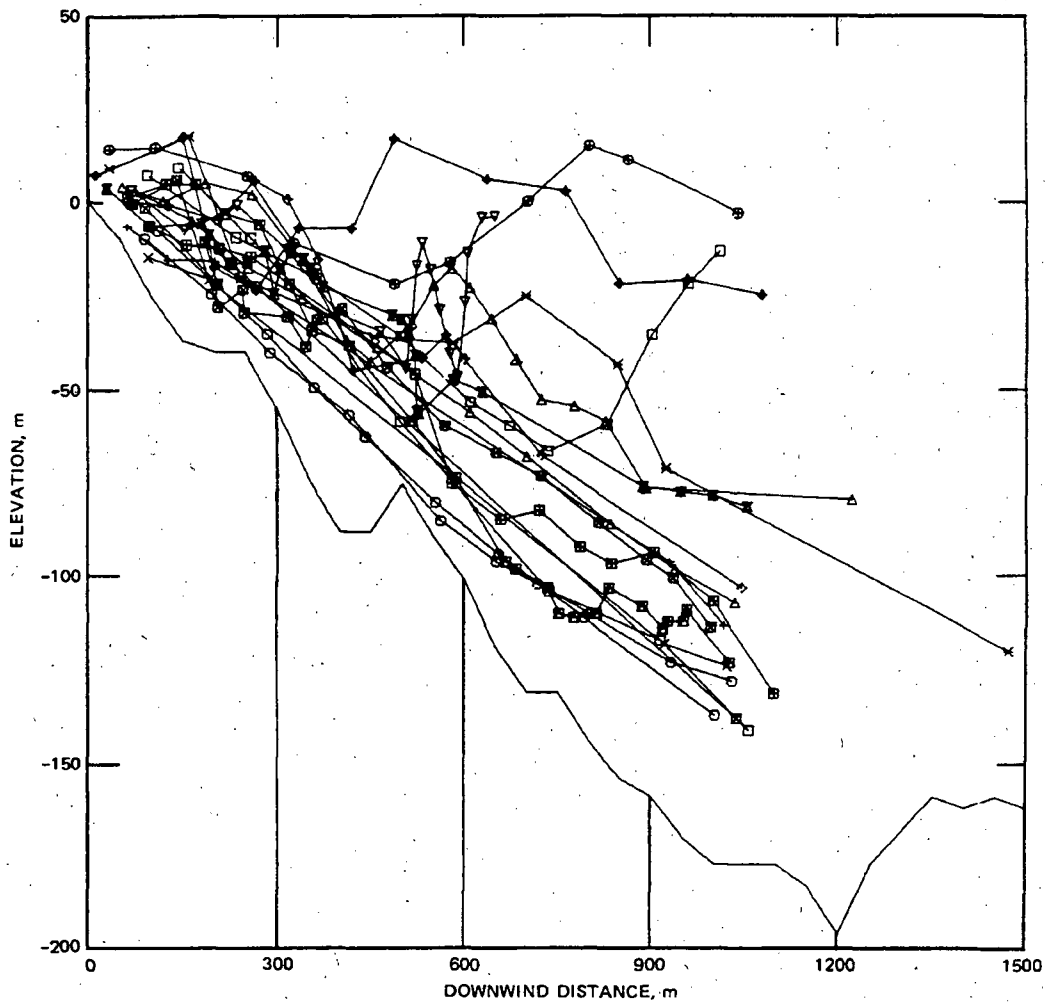

Fig. 12.5 Composite view of nighttime neutral pilot balloon trajectories down Anderson Creek canyon in the Geysers geothermal area. The solid line beneath all the trajectories is the underlying terrain elevation. Presumably the top of the drainage flow is marked by the point at which the trajectories pop up out of the flow. (From C. J. Nappo, S. R. Hanna, and H. F. Snodgrass, Drainage Wind Observations Using Neutral-Lift Balloons, in Second Joint Conference on Applications of Air Pollution Meteorology, p. 496, American Meteorological Society, Boston, Mass., 1980.)
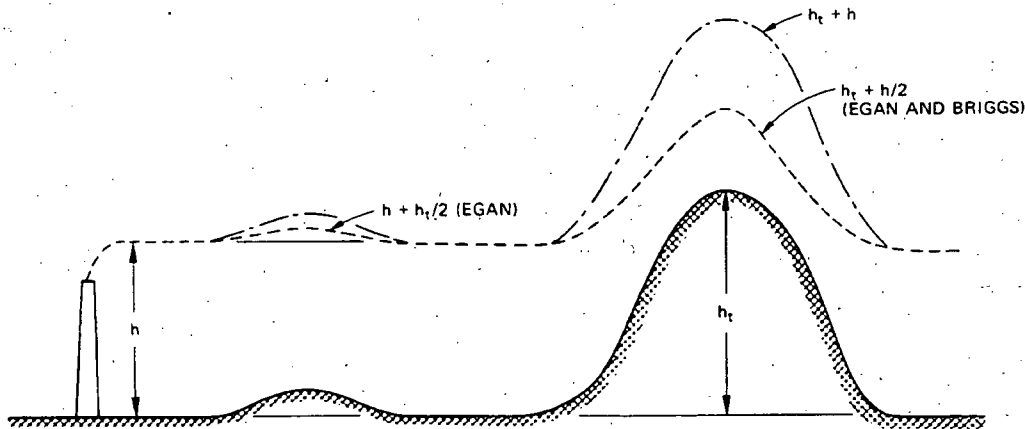
Fig. 12.6 Illustration of plume height assumptions in Briggs (1973) (———) and Egan (1975) (— — —) models for neutral and unstable conditions. The line $h_t + h$ is also shown.
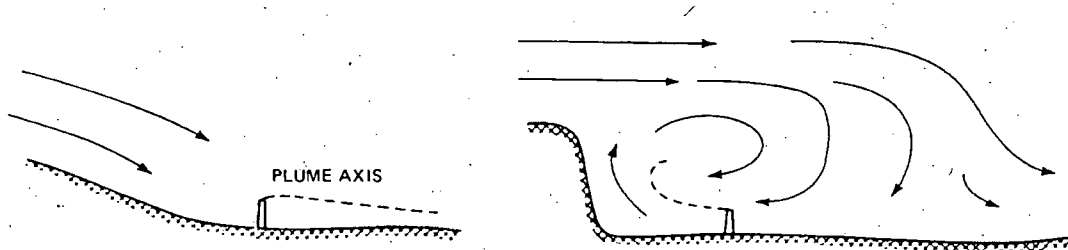

Fig. 12.7 Effect of upwind terrain on plume trajectories for gentle slopes and abrupt ridges.

situations we do not have the luxury of such detailed observations. In this case the empirical methods, which are based on models developed by Briggs (1973) and Egan (1975, 1979), described in the following paragraphs can be used to estimate diffusion from elevated point sources.

First, will a plume impact on a terrain obstacle, or will it ride up over the obstacle? If a terrain rise is downwind of a source in neutral and unstable conditions (Pasquill—Gifford classes A–B–C–D; or $F_H > 1$), the plume tends to ride up the slope while losing part of its effective stack height (h) relative to the ground. In this case Briggs (1973) suggests that h should be reduced by the terrain height (h_t) or h/2, whichever is the smallest reduction. Terrain height (h_t) is measured from the base of the source stack. This concept is illustrated in Fig. 12.6. The h/2 correction for high terrain is based on potential flow theory and wind-tunnel experiments, as mentioned in Sec. 12-2. Egan's (1975) model is the same as that of Briggs except that Egan suggests a reduction of $h_t/2$ rather than h_t for terrain heights less than half the effective plume height. Thus the assumption by Egan would give slightly lower ground-level concentrations at the surface of small hills than that by Briggs. In

stable conditions (Pasquill—Gifford classes E–F; or $F_H < 1$), both modelers assume that the plume maintains a constant elevation; thus the effective plume height (h) is reduced by terrain height (h_t). If the terrain height is greater than the effective plume height, the plume may impinge on it in E or F conditions.

If there is a terrain rise upwind of the source and the average slope of the rise above the source exceeds 2%, downwash may be induced by the air flowing down over the terrain drop. For steep hills, it is possible to get a "cavity" effect, i.e., a counter-rotating eddy. The cavity would extend three to ten hill heights downwind, which would possibly cause downwash and fumigation of a plume in this region. Figure 12.7 illustrates these effects. For more precise estimates of concentration distributions in this case, wind-tunnel or water-channel modeling of the situation should be done since the trajectories depend heavily on details of the topography.

Chapter 4 shows that an image source can be used in the Gaussian plume model to account for "reflection" from the ground surface. However, Egan et al. (1979) point out that this assumption leads to an abrupt factor of 2 increase in axial plume concentra-
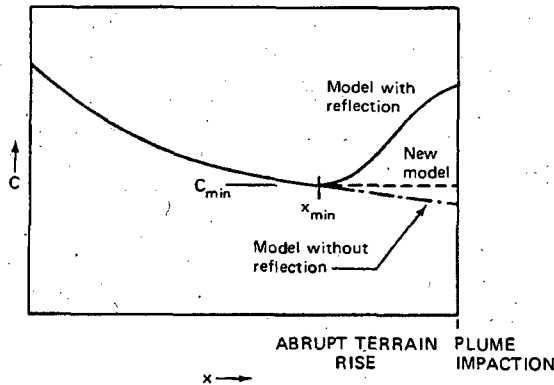
Fig. 12.8 Axial concentration variation with downwind distance as an abrupt terrain rise is approached. ——, Gaussian model with reflection. — · —, Gaussian model without reflection. — — —, recommended curve.

tion from plumes impinging on steep terrain in stable (E–F; $F_H < 1$) conditions. Therefore his model has the requirement that axial plume concentration can never increase with downwind distance (see Fig. 12.8). For this model to be applied, the solid curve in the figure must first be calculated so that the minimum concentrations (C_{min}) at point x_{min} can be determined. From point x_{min} to the point at which the plume strikes the terrain, the axial concentration is assumed to equal C_{min}.

The analysis of σ_θ observations in complex terrain at the Geysers geothermal site described in Sec. 12-2 showed that σ_θ was close to what would be expected over flat terrain during the day; however, owing to terrain effects, it was enhanced during the night. In fact, nighttime σ_θ does not fall much below the "neutral" value. This result is consistent with the few limited diffusion experiments that have been conducted in complex terrain and supports the assumption by Egan et al. (1979) that stable classes E and F should be shifted to neutral class D when selecting σ_y and σ_z. Knowledge of the site (e.g., valley width) should be used to modify σ_y if necessary. During neutral and unstable conditions, flat-terrain σ_y and σ_z curves can be used.

Diffusion in valleys is limited when the valley width (W) equals roughly $2\sigma_y$. At night elevated plumes could fill up the valley horizontally with very little vertical diffusion (see Fig. 12.9). The highest concentration experienced by the valley walls would be given by

$$C = \left(\frac{2}{\pi}\right)^{\frac{1}{2}} \frac{Q}{\sigma_z u W} \qquad (12.7)$$

In the morning, "break-up fumigation" brings the pollutant to the valley floor when the stable layer is eroded from below by the heating of the ground. The average concentration in this case is
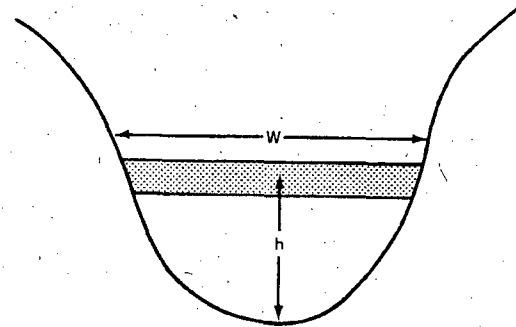

Fig. 12.9 Schematic view of an elevated plume mixed across a valley of width W during stable conditions.

$$C = \frac{Q}{uhW} \qquad (12.8)$$

where all variables are nighttime values.

Problems

1. A highway follows a constant elevation contour along the side and very near the top of a two-dimensional slope with an angle of 10°. Carbon monoxide emissions are 0.1 g sec^{-1} m^{-1}. Assume night conditions with a drainage wind of 1 m/sec. If the carbon monoxide mixes uniformly within the drainage layer, what is the carbon monoxide concentration a distance of 200 m, 500 m, and 1000 m down the slope from the highway?

2. Consider an isothermal atmosphere with a wind speed of 5 m/sec flowing over a hill of height 200 m. Calculate the internal Froude number. What will happen to a plume heading toward the hill?

3. With the use of Briggs's criteria, fill in the following table. Assume neutral conditions.

Plume rise above level terrain (h), m	Hill height (h_t), m	Predicted height of plume above hill
200	10	
10	9.9	
100	200	
500	1000	
0	100	

4. Assume that an elevated point-source plume will impact a steep mesa during very stable conditions. The source strength is 10 g/sec and the wind speed is 4 m/sec. Calculate the centerline concentration at the point the plume impacts the mesa a distance of 5 km from the source.